Earth and Planetary Science Letters 351-352 (2012) 208–214

Contents lists available at SciVerse ScienceDirect

Earth and Planetary Science Letters

journal homepage: www.elsevier.com/locate/epsl

The formation of mountain range curvature by gravitational spreading

Alex Copley

COMET+, Bullard Labs, Department of Earth Sciences, University of Cambridge, Cambridge, UK

ARTICLE INFO

Article history:
Received 14 May 2012
Received in revised form
25 July 2012
Accepted 26 July 2012
Editor: P. Shearer

Keywords:
mountain range curvature
continental tectonics
lithosphere rheology

ABSTRACT

This paper presents a mechanism by which mountain ranges can form curved range-fronts. Gravitational spreading of mountain ranges that have been thrust onto rigid lowlands will result in the formation of curvature, provided that enough gravity-driven flow occurs to dominate the shape of the topography. Whether this mechanism can operate during the lifetime of a given mountain range depends upon the viscosity of the range, the square of the along-strike length of the range, and the cube of the elevation of the range. The curvature of the southern edge of the Tibetan Plateau is consistent with formation by gravitational spreading provided that the viscosity is similar to that previously estimated using other, independent, methods. The low elevation and young age of the Zagros mountains mean that large-scale curvature has not had time to develop. The short along-strike extent and possibly low viscosity of the Sulaiman Ranges in Pakistan may have allowed the ranges to form their distinctive arcuate shape. The formation of range-front curvature plays an important role in controlling the tectonic evolution of the interiors of the ranges, with arc-parallel extension becoming progressively more important as range-front curvature develops.

1. Introduction

The study and interpretation of plan-view curvature in mountain ranges has a long history (e.g. Suess, 1909; Argand, 1924; Carey, 1955). This topic is central to our understanding of the evolution of topography and deformation within the continents, and therefore is important in studies of continental rheology, tectonics, and the interpretation of the geological record of mountain building (e.g. Platt et al., 1989; Hindle and Burkhard, 1999). A variety of mechanisms have been proposed for generating curvature in mountain ranges (also known as the formation of 'oroclines'), as summarised in Marshak (2004). The majority of previous suggestions have appealed to along-strike changes in foreland basins (e.g. lateral variations in sediment thickness), in thrust belt decollement properties, or in the geometry or motion of crustal blocks bounding mountain ranges. This paper presents an alternative method by which mountain ranges can form curved range-fronts: by the gravitational spreading of the material forming the range. This mechanism can be expected to be important whenever the crustal thickness and viscosity of a mountain range allow significant gravity-driven flow to occur (as quantified below). Previous studies have also suggested that gravitational driving forces may play a role in the development of mountain range curvature (e.g. Merle, 1989; Platt et al., 1989), and the main aim of this paper is to construct a numerical model that allows the timescales involved, and the factors that control the behaviour, to be quantified. Gravitational spreading is not suggested as a replacement for the earlier views on the formation of mountain range curvature, but as an alternative, which it is argued below is more consistent with observations of some mountain ranges.

2. Dynamic models of mountain ranges

A variety of dynamic models have previously been published that describe the evolution of mountain ranges. One popular class of models is based on the 'thin-viscous-sheet' formulation of England and McKenzie (1982), which has been widely applied (e.g. England and Houseman, 1986; Hsui et al., 1990; Flesch et al., 2001; Jimenez-Munt et al., 2005). This model assumes that there are negligible shear-stresses exerted on the base of the flowing layer, which is likely to be the case in the interiors of some mountain ranges. However, the margins of many mountain ranges worldwide are characterised by the underthrusting of relatively strong material beneath the ranges (e.g. peninsular India beneath the southern Tibetan Plateau, e.g. Nabelek et al., 2009; the Brazilian Shield beneath the eastern margin of the central Andes, e.g. Lamb and Hoke, 1997; and Arabia beneath the Zagros mountains of southwest Iran, e.g. Nissen et al., 2011). In such a situation, if the underthrusting plate retains its strength where it underlies the mountain range (e.g. Copley et al., 2011), it will provide a rigid lower boundary to the deformation in the overlying crust. In this situation, significant shear-stresses on

E-mail address: acc41@cam.ac.uk

0012-821X/$ - see front matter © 2012 Elsevier B.V. All rights reserved.
http://dx.doi.org/10.1016/j.epsl.2012.07.036

horizontal planes are transmitted between the underthrusting plate and the overlying mountain range. Therefore, in regions of large-scale underthrusting of rigid material, the solutions of 'thin-viscous-sheet' calculations are not applicable. Because this paper is concerned with the generation of curvature at the range-fronts of mountain ranges, where such underthrusting is common, a model will be used which differs from the 'thin-viscous-sheet' model by considering shear-stresses on horizontal planes.

A variety of other models of mountain range evolution have been constructed in cross-section, using a range of different rheologies and boundary conditions (e.g. Zhao and Morgan, 1987; Clark and Royden, 2000; Beaumont et al., 2004; Bendick et al., 2008). However, in order to quantify the rates and characteristics of range-front curvature, it is necessary to construct models of mountain ranges that include both horizontal dimensions. This paper will therefore describe a model that includes these dimensions, and allows the timescales relating to the formation of range-front curvature to be quantified.

In order to allow dynamic models to be constructed, and to keep the models simple enough to allow expressions to be obtained for the quantities of interest, the model described below follows many previous authors in assuming a fluid rheology (e.g. England and McKenzie, 1982; Houseman and England, 1986; Flesch et al., 2001). Such models are clearly unable to reproduce detailed features of the surface deformation on the scale of individual faults in the upper crust. However, considerable progress has been made by constructing fluid dynamical models to study the large-scale deformation in regions where ductile deformation beneath the brittle upper crust is important, or where pressure-solution creep in thick piles of sediment accommodates the deformation, and for these reasons a fluid rheology is used here. A constant viscosity has been used throughout, which means that the viscosities discussed below should be considered as a representation of the bulk properties of the mountain ranges.

3. Mountain ranges viewed as gravity currents

In order to study regions where large-scale underthrusting of rigid material is observed on the margins of mountain ranges (e.g. Nabelek et al., 2009; Lamb and Hoke, 1997; Nissen et al., 2011), a model has been constructed in which a mountain range has a rigid lower boundary (which represents the underthrust rigid crust of the bounding plate). The difference in gravitational potential energy between mountains and lowlands means that the mountains will deform to reduce their potential energy, which results in lateral spreading above this rigid lower boundary. Lateral motion in response to gravitational driving forces is termed a 'gravity current', and the phenomenon of gravity currents propagating over rigid lower boundaries has been extensively documented in the fluid dynamics literature (e.g. Huppert, 1982). Recent work has suggested that the present-day tectonics of southern Tibet can be viewed as a gravity current spreading over the rigid underthrust Indian lower crust (e.g. Copley and McKenzie, 2007; Copley et al., 2011). Such a model can reproduce the observed rates of motion and sense of strain in the region. This paper investigates the implications of such behaviour for the evolution through time of mountain ranges.

The theoretical basis for the propagation of gravity currents over a rigid base was detailed by Huppert (1982). If an irregularly shaped pile of fluid is placed upon a rigid base and allowed to flow (e.g. honey on a glass plate), it will eventually assume an axi-symmetric shape. When applied to the situation of a mountain range propagating over a rigid underthrust plate, this result implies that mountain ranges will eventually form curved range-fronts. Whether this actually occurs in nature will depend upon two factors. Firstly, arguments based on a mountain range acting as a gravity current will only apply if the gravitational driving forces are the most important forces acting on the belt. Other forces, such as those relating to lateral variations in decollement properties or in the motions of the crustal blocks bounding a range, could conceivably overwhelm the effects of gravity-driven flow, implying that not all curved mountain range-fronts may result from gravitational spreading (e.g. Marshak, 2004). Secondly, the thickness and viscosity of the crust overlying the rigid underthrust lithosphere will determine whether flow can occur rapidly enough for the edge of a range to become appreciably curved during the lifetime of the mountain belt. To address this point, this paper describes numerical calculations that have been performed which allow the timings of curve formation, on the scale of the entire lengths of mountain ranges, to be estimated as a function of the geometry and material properties of the ranges. It should be noted that this paper discusses the formation of curved range-fronts in mountain ranges that are initially linear, and does not consider the reasons why some ranges may form with a curved geometry, or discuss locations in which initially curved ranges have developed even greater degrees of curvature (e.g. Barke et al., 2007).

4. Model of curvature formation

4.1. Model setup

This section describes a numerical model that allows the factors controlling the rate of curve formation on the edges of mountain ranges to be quantified. The model setup is shown in Fig. 1. A mountain range with an initial along-strike length of l is emplaced in one corner of the model domain. The $x=0$ model boundary acts as a plane of reflection, so the model represents half of a mountain range of length $2l$. The across-strike width of the initial topography is small compared with the along-strike length. Provided this is the case, the initial across-strike width has a negligible effect on the model behaviour. Likewise, the details of the shape of the topographic taper at the end of the range are unimportant.

The topography on the $y=0$ boundary in Fig. 1 is kept at the initial value within the range $0 < x < l$. This situation is equivalent to there being a reservoir of crustal material within the interior of a mountain range, beyond the extent of rigid underthrusting, that can flow onto the underthrusting plate (e.g. crust from north Tibet flowing into southern Tibet and over-riding the underthrust

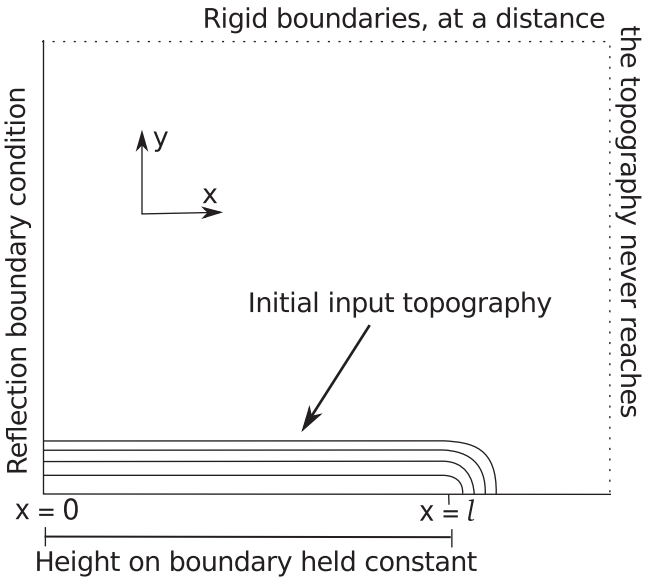

Fig. 1. Plan view of the model setup.

Indian plate, or material from the central Andes over-riding the underthrust Brazilian shield and moving into the sub-Andes). This reservoir of material is, in effect, the high topography that is created by shortening infront of the underthrusting plate as it plunges beneath the mountains. There is, in general, no step in topography observed in mountain ranges above the nose of the underthrusting plate (e.g. in central Tibet or the central Andes), indicating that this reservoir of crustal material exists in nature and can therefore be sensibly incorporated into the model. For a given driving force and viscosity, the velocities in a flow will depend upon the distance to the nearest rigid boundary (e.g. an underthrusting plate or the lowlands bordering a mountain range) (e.g. Copley, 2008). The thickness of the lithosphere is much less than the lateral extents of large mountain ranges. Therefore, flow over an underthrusting plate is expected to be slower than the rate at which it is possible to add material to the margin by flow over a stress-free base in the interior of the range, beyond the limit of underthrusting. In this situation, the reservoir of crustal material in the range interior will be able to sustain the spreading of the margin.

In the model, the topography behaves as a gravity current, and propagates across the model domain. Rigid boundary conditions (where no topography is allowed to form) are imposed at high values of x and y, but these are placed far enough from the initial topography that the model mountain ranges do not reach them during the course of the calculations, and they have no effect upon the model results.

Huppert (1982) showed that where the lateral extent of a gravity current over-riding a rigid base (where the horizontal velocity is forced to be zero) is large compared with its thickness, vertical planes deform by simple shear and the motions are governed by the local topography and the drag from the rigid lower boundary. This local balance of forces means that velocity boundary conditions are not required on the lateral edges of the model domain, and the tectonic forces produced by motions of the bounding plates are not directly felt by the material overlying the rigid underthrust plate. In this situation the equations for Newtonian fluid flow in the absence of inertial forces can be written as

$$\nabla h = \frac{\eta}{\rho g}\frac{\partial^2 \boldsymbol{u}}{\partial z^2} \tag{1}$$

where h is the surface elevation, $\boldsymbol{u}=(u,v)$ is the horizontal velocity vector, η is the viscosity, ρ is the density, z is the vertical co-ordinate, and g is the acceleration due to gravity. This equation has been non-dimensionalised using the length-scale H, which is the height of the topography held constant at $y=0$ and $0<x<l$ (Fig. 1). Lacking a natural choice for a velocity to use in the non-dimensionalisation, the velocity term has been non-dimensionalised using $\eta/\rho H$, which has units of m/s. The isostatic compensation of mountain ranges needs to be taken into account. Following McKenzie et al. (2000), g is replaced with the expression $g(f+1)^2$, where f is given by $\rho_1/(\rho_2-\rho_1)$, and ρ_1 and ρ_2 are the densities of the flowing layer and substrate, respectively. The model can then be constructed with a horizontal base, but the added factor of $(f+1)^2$ will simulate the presence of an isostatically compensated root beneath the model topography. Specifically, the surface velocity and the component of the volume flux that contributes to changes in surface elevation (rather than the deepening of the crustal root), are the same as in calculations where the root is directly modelled. The non-dimensionalised equation is then given by

$$\nabla' h' = \frac{\eta^2}{H^3\rho^2 g(f+1)^2}\frac{\partial^2 \boldsymbol{u}'}{\partial z'^2} \tag{2}$$

where primes denote non-dimensionalised quantities. This equation is solved using the method of Huppert (1982) to give the profile of velocity with depth at each point on a numerical grid. The evolution of topography at each time-step is then calculated by re-writing the incompressibility condition as a diffusion equation (e.g. Pattyn, 2003), which is solved using the finite difference method. The $x=0$ model boundary is treated as a plane of reflection when performing these calculations, as is the $y=0$ boundary at $x>l$. Material effectively flows into the model across the $y=0$ boundary at $0<x<l$, in order to keep the range at a constant elevation along this segment of the boundary.

A useful property of a low-Reynolds-number gravity current propagating over rigid base, as studied here, is that the rate of advance of the current is limited by the rate at which material from the interior of the current can flow to the nose, and not by the conditions at the nose itself (Huppert, 1982). This property means that the absence in the model of thrust faults at the nose of the range does not invalidate the results regarding the rate at which the range propagates, which will be determined by the conditions in the ductile interior of the range, where it flows over the underlying rigid plate.

In the model setup described here, there are only two parameters that can be varied: l, the half-length of the mountain range at the time of initial overthrusting (which is non-dimensionalised as $L=l/H$), and the factor $\eta^2/H^3\rho^2 g(f+1)^2$ from Eq. (2), which is hereafter referred to as α.

The model used here differs from that of Hsui et al. (1990), who also studied curve formation by gravitationally driven fluid flow. Hsui et al. (1990) used the 'thin-viscous-sheet' formulation, whereas this paper describes a model applicable to flow over a rigid underthrust plate (Section 2). Additionally, Hsui et al. (1990) 'pinned' the topography at the along-strike ends of the mountain ranges, in order to develop curved topography. The model presented here allows the topography at the ends of the range to evolve as it does elsewhere in the model domain.

4.2. Model results

Fig. 2 shows the evolution through time of one of the model mountain ranges. The mountain range progressively over-rides the lowlands, behaving as a gravity current. The plan-view curvature of the range progressively develops through time. The radius of curvature of a given contour never becomes exactly the same all the way along the range, because the act of holding part of the $y=0$ axis at a constant elevation introduces an asymmetry into the behaviour. The model topography shows the steep topographic front and gently sloping top characteristic of a gravity current propagating over a rigid base, which Copley and McKenzie (2007) suggested explained the large-scale topography of southern Tibet. The rate of propagation of the range in Fig. 2 decreases through time. This decrease is due to the rate of mass flux into the model domain, through the $y=0$ boundary at $0<x<l$. This mass flux depends upon the surface slope at $y=0$, which gradually decreases as the current propagates (Fig. 2). This gradually decreasing mass influx is then spread over a progressively larger area as the current advances, because of geometrical spreading. In a situation where the mass influx were held constant, or the lateral extent of mass influx (l) were increased through time, the rate of propagation of the range-front would be more constant. Tectonic models suggest that, in order to re-create the strain observed at the present-day, there is a compressive force transmitted from northern Tibet to southern Tibet through the upper crust (Copley et al., 2011). Such a force is not present in the models presented here, and would increase the rate of mass influx. In order to maintain the simplicity of the models, forces of this nature have not been considered further, but it should be noted that this means the viscosities presented below, and the timescales required to attain curvature, should be taken as lower and upper bounds, respectively.

Models equivalent to Fig. 2 have been run for a range of values of α and the initial mountain belt half-length (l). It is then possible

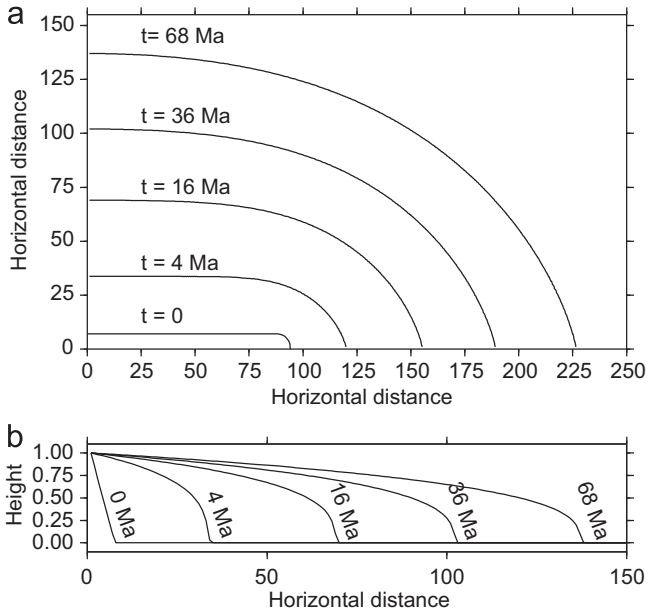

Fig. 2. (a) Plan view of the evolution through time of a range where $\alpha = 1 \times 10^{19}$, and times are dimensionalised assuming $H = 5$ km, $\rho = 2800$ kg/m^3, and $\eta = 8 \times 10^{19}$ Pa s. The lines are contours representing 10% of the maximum elevation, which effectively shows the position of the range-front. Distances are given as multiples of H. (b) The variation in model topography along the line $x = 0$.

to quantitatively investigate the time taken to reach a situation in which the radius of curvature varies by less than a given factor between the different parts of the range. It is found from the numerical experiments that this time is given by $T = \beta\alpha L^2$ in non-dimensionalised variables, which is

$$t = \frac{\beta\eta l^2}{h^3\rho g(f+1)^2} \tag{3}$$

in the dimensional equivalents. β is a constant, the value of which depends upon the degree of curvature of interest. If the radius of curvature of the section of mountain range at $0 < x < l$ is compared with the radius of curvature of the range at $x > l$, then β is 4.6 if the calculated time represents when the two radii differ by less than a factor of 4. If this factor of 4 is replaced by factors of 2, 1.5, and 1.3, then β takes the values of 11.0, 21.9, and 33.3, respectively.

When applying Eq. (3) to mountain ranges, it should be noted that it is not immediately clear what value should be used for l, the initial along-strike half-length of the range. In the model, l represents the along-strike half-length of the initial overthrusting onto the rigid lowlands. The model mountain range then grows along-strike, as well as across-strike. Viewing a range at the present-day, it is difficult to know what geometry the initial overthrusting had, so caution should be used when deciding upon the value of l when using Eq. (3).

4.3. Lateral variability

The model described above simulated a mountain belt with no lateral variations in material properties. However, it is worth considering the effects that along-strike variability in rheology may have, as these variations may be found in the natural world. Numerical experiments have been performed in which the initial input topography is the same along the entire length of the $y = 0$ axis, and only depends upon the y co-ordinate (i.e. is the same as in the range $0 < x < l$ in Fig. 1). The boundary condition on the right-hand model boundary has then been modelled in the same manner as the $x = 0$ boundary, as a reflective boundary condition. In this situation, the topography propagates parallel to the y-axis, there is no along-strike variability, and curvature does not form. In a modification of this model, the value of the parameter α has been reduced in the domain $0 < x < l$, and in material which flows out of this region, in order to simulate the presence of along-strike changes in rheology. In the situation where the contrast in α is large, the motion of material that originates in the region $x > l$ is small compared with that originating at $0 < x < l$, and the results are similar to those presented above. As the lateral contrast in α becomes smaller, the material originating at $x > l$ propagates parallel to the y-axis, and the lateral extent of the curved part of the range decreases.

4.4. Interaction with other mountain ranges

In some areas, such as the eastern and western ends of the Himalaya, mountain ranges come into contact with other ranges that have different strikes and are propagating in different directions (such as the junction between the eastern Himalayas and the Indo-Burman Ranges at the East Himalayan Syntaxis; Fig. 3a). It is therefore worth considering what effect such interactions will have on the model results. Fig. 4 shows the results of a calculation identical to the original model described above, except for the addition of a second mountain range which begins at the right-hand edge of the model domain in Fig. 1 and propagates leftwards, parallel to the x-axis. Fig. 4 shows the positions of the range-fronts of the mountain ranges, before and after they come into contact, as solid black lines. The model results from equivalent times in the original model are shown as grey dashed lines. The behaviour of a gravity current propagating over a rigid base is dominated by the balance of local stresses, related to topography and the drag from the rigid base. The interaction of the along-strike end of a mountain range with a neighbouring range therefore does little to affect the behaviour of the central part of the range, as is demonstrated by Fig. 4. It is therefore possible to apply the model results described above to mountain ranges that are now in contact with neighbouring belts. Furthermore, the behaviour shown in Fig. 4 provides an explanation for the formation of syntaxes between mountain ranges, as previously suggested by Copley and McKenzie (2007) for the Eastern Himalayan Syntaxis.

5. Comparison with observations

Having estimated the timescales required for mountain belts to attain curved range-fronts by gravitational spreading, this section compares the estimated timescales to observations from some mountain ranges.

5.1. A large and curved mountain range: the Tibetan Plateau

The southern margin of the Tibetan plateau is curved (Fig. 3a), and geological reconstructions and rotations measured using palaeomagnetism (as collated in van Hinsbergen et al., 2011) show that this curve has formed since the onset of mountain building in the region. Lateral changes in the curvature of the range do not correspond to variations in sediment thickness in the foreland basin, the arc-normal surface motion measured using GPS is roughly constant along the length of the range (e.g. Banerjee et al., 2008), and there are no clear along-strike differences in the seismicity of the range-front. Lateral changes in basin or decollement properties therefore do not explain the curvature of the southern margin of Tibet, which is instead likely to be due to the gravitational spreading of Tibet over the rigid Indian crust

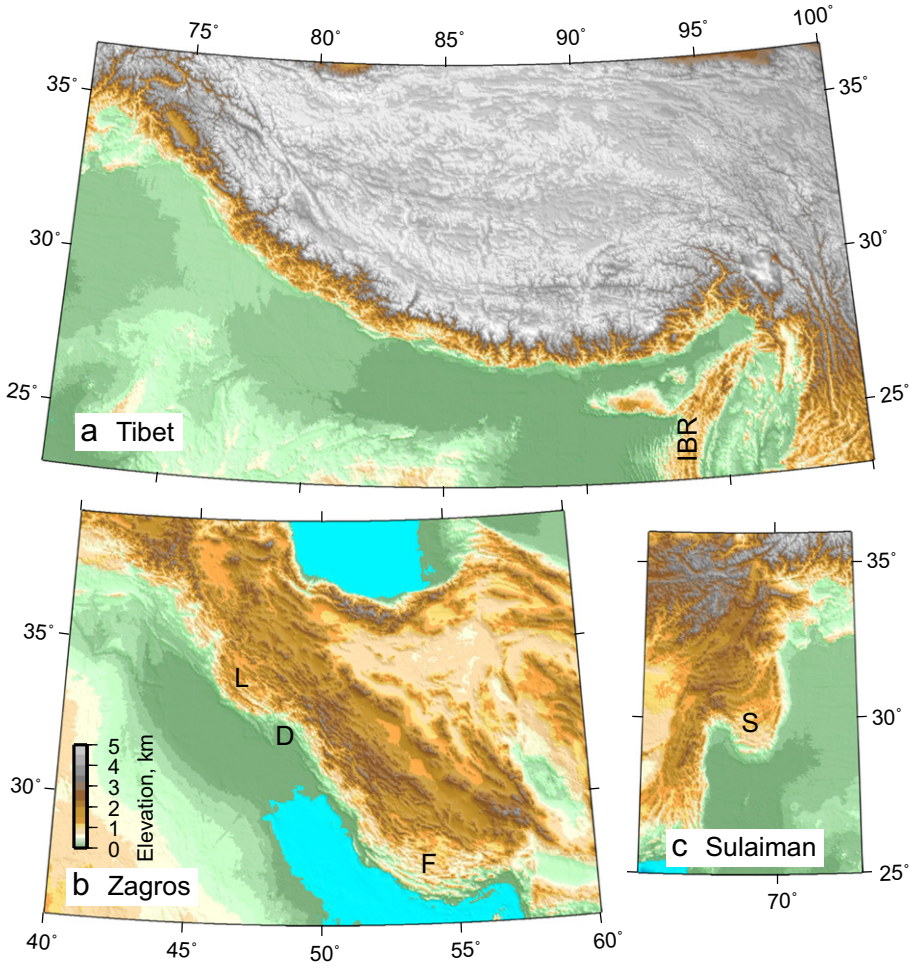

Fig. 3. Topography of the southern Tibetan Plateau, the Zagros Mountains of Iran, and the Sulaiman Ranges in Pakistan, all shown to scale. IBR, Indo-Burman Ranges; D, Dezful Embayment; L, Lurestan Arc; F, Fars Arc; S, Sulaiman Ranges.

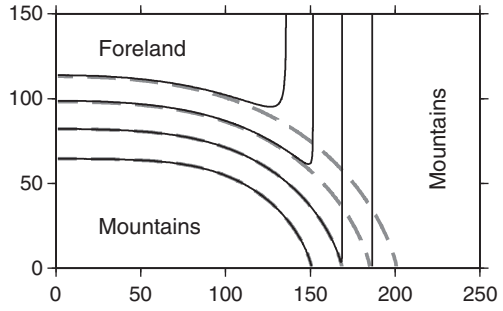

Fig. 4. The results of calculations identical to those shown in Fig. 2, but with the addition of a second mountain range propagating leftwards parallel to the x-axis. The solid lines show the positions of the range-fronts of the mountain ranges and the grey dashed lines show those from the original model at equivalent times.

(which also explains the present-day tectonics of the region, e.g. Copley et al., 2011).

The time elapsed since continent–continent collision, and the degree of curvature observed, can be used to estimate the viscosity of the mountain range. The current continent–continent collision is thought to have begun at ~ 50 Ma (e.g. Dupont-Nivet et al., 2010; Copley et al., 2010, and references therein), which is likely to represent the initial age of overthrusting onto the Indian plate. West of $\sim 90^{\circ}$E longitude, the southern margin of the Tibetan Plateau forms a curve with a roughly constant radius of curvature (Bendick and Bilham, 2001). East of $\sim 90^{\circ}$, the radius of curvature is ~ 4 times lower. Using Eq. (3), if the along-strike half-length of initial overthrusting is taken to be between 500 and 1000 km, we can estimate the viscosity to be between 3×10^{20} and 8×10^{19} Pa s, respectively (assuming that $f=7$, (Copley and McKenzie, 2007), $h=5$ km, and $\rho = 2800$ kg/m^3). This value is consistent with viscosity estimates based upon the present-day tectonics of southern Tibet (10^{20} Pa s; Copley and McKenzie, 2007), confirming that gravitational spreading is a viable mechanism for the formation of curvature on this margin of the Tibetan Plateau.

5.2. A large and straight mountain range: the Zagros Mountains

In contrast to southern Tibet, the majority of the length of the Zagros mountains shows little curvature (Fig. 3b). West of $\sim 52^{\circ}$E longitude, the mountain range is approximately linear, and the minor deviations such as the Dezful Embayment and Lurestan Arc (D and L in Fig. 3b) have an across-strike amplitude that is small compared with the along-strike length of the range. East of this, the range curves towards its termination in the region of the Fars Arc (F in Fig. 3b). This shape, with a mostly straight range-front and a curve at the end of the range, is as expected at times early in the process of curve formation (Fig. 2).

Estimates for the age of continent–continent collision in Iran vary between 10 and 35 Ma (e.g. McQuarrie et al., 2003; Allen and

Armstrong, 2008). If the along-strike half-length of the range is taken to be 800 km, the viscosity of the range would have to be the improbably low value of 3.7×10^{18}–1.3×10^{19} Pa s in order for significant curvature to have formed along the length of the range since collision began (assuming $h=2.5$ km, $f=8$, $\rho=2800$ kg/m^3). This lack of curvature results from both the relative youth of the range compared with Tibet, and also the lower topography (Eq. (3)).

5.3. A small and curved mountain range: the Sulaiman Ranges

The above analysis of the Tibetan Plateau suggested that mountain ranges with a large crustal thickness can form curved range-fronts within the typical lifespans of orogenic belts. It is possible that ranges with lower crustal thicknesses can also form curved range-fronts by gravitational spreading, but would require considerably more time, a lower viscosity, or a shorter along-strike length in order to achieve the same degree of curvature (Eq. (3)). A possible example of a curved mountain range-front that has formed because of both a low viscosity and a small along-strike length is the Sulaiman Ranges in Pakistan (Fig. 3c).

Macedo and Marshak (1999) previously suggested that the arcuate shape of the range may have formed because of propagation into a foreland basin of variable depth. An alternative mechanism is that the short length and potential low viscosity of the ranges (due to being composed of a thick pile of sediments, rather than crystalline basement, e.g. Banks and Warbutron, 1986) may have allowed gravitational spreading of the topography into an arcuate shape. The radial directions of slip-vectors in thrust-faulting earthquakes on the margins of the range (Bernard et al., 2000) lend support to this hypothesis, because such behaviour is expected if gravitational spreading is occurring. Such a mechanism requires that the Sulaiman Ranges are weaker than the adjacent mountains on the margin of the Indian Plate to the north and south, otherwise the entire mountain range-front would advance in line and no curve would form (Section 4.3). Eq. (3) suggests that the curvature of the Sulaiman Ranges could form since India collided with Asia if the viscosity of the range were $\sim10^{20}$ Pa s. Unfortunately, the lack of information regarding the present-day surface velocities in the region prevents a comparison between this viscosity estimate and one calculated to be consistent with the present-day tectonics. However, the Indo-Burman ranges overthrust the eastern margin of the Indian plate (IBR in Fig. 3a), and have a similar lithology and elevation to the Sulaiman Ranges, and in this region Copley and McKenzie (2007) estimated the viscosity to be 10^{19}–10^{20} Pa s; comparable to that required to explain the curvature of the Sulaiman Ranges.

With the information presently available to us we cannot conclusively state whether gravitational spreading or lateral variations in foreland basin properties (Macedo and Marshak, 1999) better explain the formation of curvature in the Sulaiman Ranges. It is possible that both may be simultaneously operating, by gravitational spreading into a basin of variable depth. However, the gravitational spreading hypothesis is viable, and demonstrates the principle that small mountain ranges with low viscosities could conceivably develop range-front curvature by the same mechanism as large ranges.

6. Discussion

The numerical models presented above demonstrate that a mountain range that is emplaced upon strong crust will form a curved margin provided that enough gravity-driven flow can occur in order to dominate the shape of the topography. The time taken for a given amount of curvature to be attained depends upon the viscosity of the range, the along-strike length of the initial topography, and the height of the range. Curvature can therefore be expected to form within the duration of an orogenic event if the mountain range concerned is high, because of both the importance of this parameter itself, and also because larger amounts of crustal thickening will eventually result in lower viscosities because of hotter geotherms through internal radiogenic heating (e.g. McKenzie and Priestley, 2008). Alternatively, ranges with low along-strike lengths or low viscosities may also be expected to form curved range-fronts.

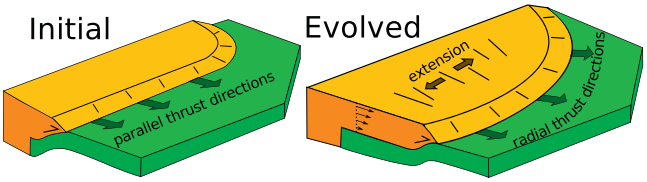

Fig. 5. Cartoon to illustrate the evolution of deformation as mountain-front curvature develops.

The formation of mountain-front curvature has implications for the strain within the interiors of mountain ranges. In situations where gravity-driven flow plays a significant role in controlling the tectonic motions, and the edge of the range is curved, extensional stresses parallel to the overall strike of the mountain belt will be generated within the range (such as in southern Tibet, e.g. Armijo et al., 1986; Copley et al., 2011). These stresses will increase in magnitude as the degree of curvature of the range-front increases. The tectonics of the interiors of mountain ranges will therefore depend upon the processes which generate range-front curvature, with extensional stresses becoming increasingly important as range-front curvature increases. The onset of east–west extension in Tibet at times significantly after the date of continent–continent collision (at $\sim$20 Ma, e.g. Mitsuishi et al., 2012, and references therein), may record the time-delay required for significant range-front curvature to develop (Fig. 5).

The formation of mountain front curvature by gravitational spreading may be visible in the geological record. Transport directions would appear to fan outwards from the centre of the range, and be perpendicular to the local strike of the range-front. If the time evolution of deformation is known, the fanning out of the transport directions would be expected to increase through time as the curve at the range-front evolves. The divergence of transport directions would begin at the lateral end of the mountain range, and then propagate towards the centre of the range. In addition, arc-parallel extension would begin within the range interior at times coincident with the appearance of divergent transport directions (Fig. 5).

7. Conclusions

This paper has described a mechanism by which mountain ranges can form curved range-fronts by gravitational spreading. Whether this mechanism can operate during the lifetime of a mountain range depends upon the viscosity and range geometry (the square of the along-strike length of the range and the cube of the elevation of the range). Gravitational spreading is consistent with the formation of the curved southern margin of the Tibetan Plateau and the arcuate Sulaiman Ranges, and with the lack of large-scale curvature in the Zagros mountains. The development of range-front curvature has an important role to play in controlling the tectonic evolution of the interiors of mountain ranges.

Acknowledgements

The author is supported by a research fellowship at Pembroke College in the University of Cambridge, thanks James Jackson and

Dan McKenzie for useful discussions, and thanks Arlo Weil, one anonymous reviewer, and the Editor for comments on the manuscript.

References

Allen, M.B., Armstrong, H.A., 2008. Arabia–Eurasia collision and the forcing of mid-Cenozoic global cooling. Palaeogeogr. Palaeoclimatol. Palaeoecol. 265, 52–58.

Argand, E., 1924. La Tectonique de l'Asie. Hafner Press, New York. (Translated by A.V. Carozzi (1977)).

Armijo, R., Tapponnier, P., Mercier, J., Han, Tonglin, 1986. Quaternary extension in southern Tibet: field observations and tectonic implications. J. Geophys. Res. 91, 13803–13872.

Banerjee, P., Burgmann, R., Nagarajan, B., Apel, E., 2008. Intraplate deformation of the Indian subcontinent. Geophys. Res. Lett. 35 , http://dx.doi.org/10.1029/2008GL035468.

Banks, C.J., Warbutron, J., 1986. 'Passive-roof' duplex geometry in the frontal structures of the Kirthar and Sulaiman mountain belts Pakistan. J. Struct. Geol. 8, 229–237.

Barke, R., Lamb, S., MacNiocaill, C., 2007. Late Cenozoic bending of the Bolivian Andes: new paleomagnetic and kinematic constraints. J. Geophys. Res. 112 , ht tp://dx.doi.org/10.1029/2006JB004372.

Beaumont, C., Jamieson, R.A., Nguyen, M.H., Medvedev, S., 2004. Crustal channel flows. 1. Numerical models with applications to the tectonics of the Himalayan–Tibetan orogen. J. Geophys. Res. 109 , http://dx.doi.org/10.1029/2003JB002809.

Bendick, R., Bilham, R., 2001. How perfect is the Himalayan arc? Geology 29, 791–794.

Bendick, R., McKenzie, D., Etienne, J., 2008. Topography associated with crustal flow in continental collisions, with application to Tibet. Geophys. J. Int. 175, 375–385.

Bernard, M., Shen-Tu, B., Holt, W.E., Davis, D.M., 2000. Kinematics of active deformation in the Sulaiman Lobe and Range, Pakistan. J. Geophys. Res. 105, 13253–13279.

Carey, S., 1955. The orocline concept in geotectonics. Proc. R. Soc. Tasmania 89, 255–288.

Clark, M.K., Royden, L.H., 2000. Topographic ooze: building the eastern margin of Tibet by lower crustal flow. Geology 28, 703–706.

Copley, A., 2008. Kinematics and dynamics of the southeastern margin of the Tibetan Plateau. Geophys. J. Int. 174, 1081–1100.

Copley, A., McKenzie, D., 2007. Models of crustal flow in the India–Asia collision zone. Geophys. J. Int. 169, 683–698.

Copley, A., Avouac, J.-P., Royer, J.-Y., 2010. The India-Asia collision and the Cenozoic slowdown of the Indian plate: implications for the forces driving plate motions. J. Geophys. Res. 115, http://dxdoi.org/10.1029/2009JB006634.

Copley, A., Avouac, J.-P., Wernicke, B.P., 2011. Evidence for mechanical coupling and strong Indian lower crust beneath southern Tibet. Nature 472, 79–81.

Dupont-Nivet, G., Lippert, P.C., van Hinsbergen, D.J.J., Meijers, M.J.M., Kapp, P., 2010. Palaeolatitude and age of the Indo-Asia collision: palaeomagnetic constraints. Geophys. J. Int. 182, 1189–1198.

England, P., Houseman, G., 1986. Finite strain calculations of continental deformation. 2. Comparison with the India–Asia collision zone. J. Geophys. Res. 91, 3664–3676.

England, P., McKenzie, D., 1982. A thin viscous sheet model for continental deformation. Geophys. J. R. Astron. Soc. 70, 295–321.

Flesch, L.M., Haines, A.J., Holt, W.E., 2001. Dynamics of the India–Eurasia collision zone. J. Geophys. Res. 106, 16435–16460.

Hindle, D., Burkhard, M., 1999. Strain, displacement and rotation associated with the formation of curvature in fold belts: the example of the Jura arc. J. Struct. Geol. 21, 1089–1101.

Houseman, G., England, P., 1986. Finite strain calculations of continental deformation. 1. Method and general results for convergent zones. J. Geophys. Res. 91, 3651–3663.

Hsui, A.T., Scott Wilkerson, M., Marshak, Stephen, 1990. Topographically driven crustal flow and its implication to the development of pinned oroclines. Geophys. Res. Lett. 17, 2421–2424.

Huppert, H.E., 1982. The propagation of two-dimensional and axisymmetric gravity currents over a rigid horizontal surface. J. Fluid Mech. 121, 43–58.

Jimenez-Munt, I., Garcia-Castellanos, D., Fernandez, M., 2005. Thin-sheet modelling of lithospheric deformation and surface mass transport. Tectonophysics 407, 239–255.

Lamb, S., Hoke, L., 1997. Origin of the high plateau in the central Andes, Bolivia, South America. Tectonics 16, 623–649.

Macedo, J., Marshak, S., 1999. Controls on the geometry of fold-thrust belt salients. GSA Bull. 111, 1808–1822.

Marshak, S., 2004. Salients, recesses, arcs, oroclines, and syntaxes—a review of ideas concerning the formation of map-view curves in fold-thrust belts. AAPG Memoir 82, 131–156.

McKenzie, D., Priestley, K., 2008. The influence of lithospheric thickness variations on continental evolution. Lithos 102, 1–11.

McKenzie, D., Nimmo, F., Jackson, J., Gans, P.B., Miller, E.L., 2000. Characteristics and consequences of flow in the lower crust. J. Geophys. Res. 105, 11029–11046.

McQuarrie, N., Stock, J.M., Verdel, C., Wernicke, B.P., 2003. Cenozoic evolution of Neotethys and implications for the causes of plate motions. Geophys. Res. Lett. 30, 2036, http://dx.doi.org/10.1029/2003GL017992.

Merle, O., 1989. Strain models within spreading nappes. Tectonophysics 165, 57–71.

Mitsuishi, M., Wallis, S.R., Aoya, M., Lee, J., Wang, Y., 2012. E–W extension at 19 Ma in the Kung Co area, S. Tibet: evidence for contemporaneous E–W extension and N–S extension in the Himalayan orogen. Earth Planet. Sci. Lett. 325–326, 10–20.

Nabelek, G., Hetenyi, J., Vergne, J., Sapkota, S., Kafle, B., Jiang, M., Su, H., Chen, J., Huang, B.-S., 2009. The Hi-CLIMB Team, 2009. Underplating in the Himalaya–Tibet collision zone revealed by the Hi-CLIMB experiment. Science 325, 1371–1374.

Nissen, E., Tatar, M., Jackson, J.A., Allen, M.B., 2011. New views on earthquake faulting in the Zagros fold-and-thrust belt of Iran. Geophys. J. Int. 186, 928–944.

Pattyn, F., 2003. A new three-dimensional higher-order thermomechanical ice sheet model: basic sensitivity, ice stream development, and flow across subglacial lakes. J. Geophys. Res. 108, http://dxdoi.org/10.1029/2002JB002329.

Platt, J.P., Behrmann, J.H., Cunningham, P.C., Dewey, J.F., Helman, M., Parish, M., Shepley, M.G., Wallis, S., Weston, P.J., 1989. Kinematics of the alpine arc and the motion history of Adria. Nature 337, 158–161.

Suess, E., 1909. The Face of the Earth. Clarendon, Oxford.

van Hinsbergen, D.J.J., Kapp, P., Dupont-Nivet, G., Lippert, P.C., DeCelles, P.G., Torsvik, T.H., 2011. Restoration of Cenozoic deformation in Asia and the size of Greater India. 30, http://dx.doi.org/10.1029/2011TC002908.

Zhao, W.-L., Morgan, W.J., 1987. Injection of Indian crust into Tibetan lower crust: a two-dimensional finite element model study. Tectonics 6, 489–504.